Available online at www.sciencedirect.com
SCIENCE DIRECT®
Journal of Catalysis 224 (2004) 347–357
JOURNAL OF CATALYSIS
www.elsevier.com/locate/jcat

A novel route to produce thymol by vapor phase reaction of *m*-cresol with isopropyl acetate over Al-MCM-41 molecular sieves

K. Shanmugapriya, M. Palanichamy, Banumathi Arabindoo, and V. Murugesan *

Department of Chemistry, Anna University, Chennai-25, India

Received 22 September 2003; revised 5 March 2004; accepted 9 March 2004

Available online 20 April 2004

Abstract

Mesoporous Al-MCM-41 (Si/Al = 55 and 104) and Al,Zn-MCM-41 (Si/(Al + Zn) = 52) molecular sieves were synthesized hydrothermally. The materials were characterized by XRD, TGA, TPD (pyridine), ICP-AES, nitrogen sorption, and FT-IR techniques. The catalytic performance of these materials was examined in the vapor phase alkylation of *m*-cresol with isopropyl acetate. The products obtained were thymol, isothymol, 2-isopropyl-5-methylphenyl acetate (2-I-5-MPA), and isopropyl-3-methylphenyl ether (I-3-MPE). The time-on-stream study was carried out over Al-MCM-41(55) at 300 °C and WHSV 1.52 h^{-1} wherein optimum conversion of *m*-cresol and selectivity to thymol were obtained. The dependence of activity and selectivity on the acid sites and hydrophobic and hydrophilic properties of the catalysts is discussed.

Keywords: Acylation; Thymol; Isothymol; Al-MCM-41; Isopropyl acetate; *m*-Cresol

1. Introduction

Isopropylation of *m*-cresol continues to attract considerable attention, because one of the alkylation products, thymol, leads to menthol on hydrogenation [1–3]. Menthol has a characteristic peppermint odor and is used as a raw material for the production of antiseptic, local anesthetic, antibacterial and antifungal agents, flavors, fragrances, and preservatives [4,5]. Thymol as such exhibits activity in protecting low-density lipoproteins [6] and as an antioxidant [7–9]. It also plays an important role as intermediate in perfumery. Isopropylation of *m*-cresol with isopropyl alcohol has been already reported over oxide catalysts [10] and calcined Mg–Al hydrotalcites [11] and with propylene over acidic catalysts [12]. Activated alumina [13], γ-Al_2O_3 [14], $Al(OC_6H_5)_3$, and ZnCl-HCl [1,2] have been used as catalysts in the liquid-phase isopropylation of *m*-cresol. Y and β zeolites, ZSM-5, erionite and mordenite [15], and supported metal sulfates [1] were used in the vapor phase for such reactions. Synthetic silica–alumina and large-pore Y-type catalysts have yielded 4-isopropyl-3-methylphenol (isothymol) through isomerization and transalkylation reactions [16]. Mesoporous Al-MCM-41 molecular sieves have become catalysts in widespread use in recent years in many reactions of industrial importance. Their large pore diameter with less diffusional constraint could discourage consecutive alkylations and deactivation by coke formation. In addition, unlike zeolites, these materials could also permit simultaneous entry of many reactant molecules into the pores, thus permitting high conversion. Umamaheswari et al. [3] reported vapor phase isopropylation of *m*-cresol with isopropyl alcohol over mesoporous Al-MCM-41 molecular sieves. The selectivity of thymol was higher than that of other alkylated products.

There is a general problem in using alcohols as alkylating agents. They readily cluster around the protonic sites without dissociation to isopropyl cation. To avoid this problem esters can be substituted in the place of alcohols as reported by Umamaheswari et al. [17]. It was inferred that *tert*-butyl acetate is a better alkylating agent than the corresponding alcohol in the vapor phase reaction of *m*-cresol. Adsorption of ester through the steric free carbonyl group and subsequent liberation of *tert*-butyl cation are easily possible with ester as alkylating agent. These observations and inferences with MCM-41 have stimulated further interest in the study of the isopropylation of *m*-cresol with isopropyl acetate as

* Corresponding author. Fax: +91-44-22200660.
E-mail address: v_murugu@hotmail.com (V. Murugesan).

0021-9517/$ – see front matter
doi:10.1016/j.jcat.2004.03.019

the alkylating agent. In the present work we have investigated this reaction using Al-MCM-41 (Si/Al = 55 and 104) and Al,Zn-MCM-41 (Si/(Al + Zn) = 52) so that the influence of hydrophilic and hydrophobic properties and density of acid sites of the catalysts on conversion and product selectivity can be correlated.

2. Experimental

2.1. Preparation of catalysts

All reagents, viz., sodium metasilicate, aluminum sulfate, zinc sulfate, cetyltrimethylammonium bromide (CTAB), sulfuric acid, isopropyl acetate, and *m*-cresol were purchased from Merck and used as such. Samples of Al-MCM-41 with Si/Al = 55 and 104 and Al,Zn-MCM-41 with Si/(Al + Zn) = 52 were synthesized hydrothermally using a gel composition of SiO_2:*x* Al_2O_3:0.2 CTAB:0.89 H_2SO_4:120 H_2O (*x* varies with Si/Al and Si/(Al + Zn) ratios). In a typical synthesis, 10.6 g of sodium metasilicate in water was combined with an appropriate amount of aluminum sulfate in distilled water, and the pH of the solution was adjusted to 10.5 using 1 M sulfuric acid with constant stirring to form a gel. After 30 min, an aqueous solution of CTAB (structure directing agent) was added and the mixture was stirred for 1 h at room temperature. The resulting suspension was then autoclaved at 170 °C for about 12 h. After crystallization, Al-MCM-41 material was recovered by filtration, washed with distilled water, and dried at 80 °C for 8 h. Al,Zn-MCM-41 with Si/(Al + Zn) = 52 was also synthesized by following the same procedure using both aluminum sulfate and zinc sulfate during initial synthesis. Mesoporous Al-MCM-41 and Al,Zn-MCM-41 catalysts were obtained by removing the occluded surfactant, which filled in the pores, by calcining the samples at 550 °C in air for 6 h.

2.2. Physicochemical characterization

The powder X-ray diffraction patterns of all the samples were recorded with a Siemens D5005 Stereoscan diffractometer using nickel-filtered Cu-K_α radiation and a liquid nitrogen-cooled germanium solid-state detector. The diffractograms were recorded in the 2θ range of 0.8°–10° in steps of 0.02° with a count time of 10 s at each point. Al and Zn content of Al,Zn-MCM-41 and Al content of Al-MCM-41 were determined using inductively coupled plasma atomic emission spectroscopy (ICP-AES) with the Labtum Plasma 8440 instrument.

Fourier transform infrared spectra of the materials were recorded with a resolution of 2 cm^{-1} on a Nicolet (Avatar 360) instrument using the KBr pellet technique. About 15 mg of the sample was pressed (under a pressure of 2 tons/cm^2) into a self-supported wafer of 13-mm diameter. This pellet was used to record the infrared spectra in the range 4000–400 cm^{-1}. The acidity of the calcined materials was recorded on a Nicolet Avatar 360 FT-IR spectrophotometer equipped with a high-temperature vacuum chamber. Approximately 10 mg of the sample was taken in the sample holder and dehydrated at 500 °C for 6 h under vacuum (10^{-5} mbar). The sample was then cooled to room temperature. Then pyridine was adsorbed at room temperature. The physically adsorbed pyridine was removed by heating the sample at 150 °C under vacuum (10^{-5} mbar) for 30 min, the removed material was cooled to room temperature, and the spectrum was recorded. The acidity was calculated using the extinction coefficients of the bands of Brønsted and Lewis acid site adsorbed pyridine.

Surface area, pore volume, and pore size distribution of the materials were measured by nitrogen adsorption at 77 K with an ASAP-2010 porosimeter from Micromeritics Corporation (Norcross, GA, USA). Before nitrogen adsorption–desorption measurements, the samples was degassed at 623 K at 10^{-5} Torr and the specific area of the samples was determined from the linear portion of the BET plots. Pore size distributions were calculated from the desorption branch of N_2 adsorption–desorption isotherms using the Barrett Joyner Halenda (BJH) algorithm (ASAP-2010 built-in software from Micromeritics). Thermogravimetric analysis (TGA) and differential thermal analysis (DTA) of the materials were performed simultaneously on a high-resolution Mettler TA 3000 thermogravimetric analyzer. The samples were heated in air at a heating rate of 20 °C/min in the temperature range 25–700 °C.

^{29}Si MAS-NMR spectra were recorded in a DRX-500FT-NMR spectrometer at a frequency of 59.64 MHz, spinning speed of 8 KHz, pulse length of 2.50 μs (45° pulse), delay time of 10 s, and spectral width of 335 ppm. Two thousand scans were acquired and processed with a line broadening of 50 Hz. The chemical shifts were reported with reference to trimethylsilylpropanesulfonic acid (TSP). Solid-state ^{27}Al MAS-NMR measurements were performed on a Bruker MSL 400 spectrometer equipped with a magic-angle spinning (MAS) unit. The ^{27}Al MAS-NMR spectra were recorded at a frequency of 104.22 MHz, a spinning rate of 8 KHz with a pulse length of 1.0 μs, a delay time of 0.2 s, and a spectral width of 330 ppm. The total scans were 150 and the line broadening was 50 Hz. ^{27}Al MAS-NMR chemical shifts were reported in relation to the liquid solution of aluminum nitrate.

2.3. Catalytic performance: isopropylation of *m*-cresol

Isopropylation of *m*-cresol with isopropyl acetate was carried out in a fixed-bed, vertical-flow-type reactor made up of a borosil glass tube 40 cm in length and 2 cm in internal diameter. About 0.5 g of the catalyst was placed in the middle of the reactor and supported on either side with a thin layer of quartz wool and ceramic beads. The reactor was heated to the requisite temperature with the help of a tubular furnace controlled by a digital temperature controller cum indicator. Reactants were fed into the reactor using a

syringe infusion pump (SAGE instruments) that could be operated at different flow rates. The reaction was carried out at atmospheric pressure. The bottom of the reactor was connected to a coiled condenser and a receiver to collect the products. The products obtained in the first 10 min were discarded, and the product collected after 1 h was analyzed for identification. After each catalytic run, the catalyst was regenerated by passing moisture- and carbon dioxide-free air through the reactor for 6 h at 500 °C.

The percent conversion of *m*-cresol was analyzed in a gas chromatograph (Shimadzu GC-17A) with a flame ionization detector equipped with a 25-m capillary column (crosslinked 5% phenylmethyl polysiloxane). The liquid products were analyzed using a Perkin Elmer Auto System XL gas chromatograph with Turbo Mass Spectrometer with helium as carrier gas (1 ml/h). As the percentage conversion of *m*-cresol was higher with Al-MCM-41(55), all other experiments concerning evaluation of the performance of the catalyst were carried out only with Al-MCM-41(55). $(\mathrm{WHSV})^{-1}$ was calculated using the expression

$$(\mathrm{WHSV})^{-1} = \frac{W}{F} = \frac{\text{weight of catalyst}}{\text{weight of flow rate}}.$$

Flow rate of the reactant is varied to maintain constant $(\mathrm{WHSV})^{-1}$ during the reaction. Selectivity to products is defined as weight of each product obtained divided by the weight of starting materials consumed, normalized to 100%. Conversion is the weight of starting material consumed divided by weight of starting material normalized to 100%.

3. Results and discussion

3.1. Characterization

XRD powder diffraction patterns of as-synthesized and calcined mesoporous Al-MCM-41 ($\mathrm{Si/Al} = 55$ and 104) and Al,Zn-MCM-41 ($\mathrm{Si/(Al + Zn)} = 52$) molecular sieves are shown in Fig. 1. The XRD patterns, taken before and after calcination, confirmed the hexagonal MCM-41 phase in the sample. After calcination, the intense peak was shifted to higher 2θ values due to pore size contraction. As displayed in the figure, as-synthesized and calcined samples exhibit an intense signal at about 1.8° due to [100] plane and weak broad signals between 2.5° and 4° (2θ) due to [110], [200], and [210] planes. These peaks confirm the hexagonal mesophase of the material. The d_{100} spacing and lattice parameter (a_0) calculated as per the literature procedure are summarized in Table 1. These XRD patterns coincide with the data already reported in the literature for mesoporous aluminosilicate molecular sieves [18,19]. From ICP-AES analysis the aluminum and zinc content of Al,Zn-MCM-41(52) were found to be 0.053 and 0.057 g, respectively. The aluminum content of Al-MCM-41(55) and Al-MCM-41(104) were found to be 0.097 and 0.051 g, respectively. Under the synthesis conditions used, the crystallization reaction was nonstoichiometric and a higher Si/Al ratio was noted in the crystal [20].

Specific surface area, specific pore volume, and pore diameter (BJH method) for calcined materials are presented in Table 1. The isotherms of nitrogen adsorption for calcined materials were measured at liquid nitrogen temperature (77 K). The isotherms show well-defined stages and they coincide with those already reported in the literature [21]. It is evident from these isotherms (Figs. 2a–2c) that good mesoporous structural ordering and narrow pore size distribution are well exhibited. The surface area of the catalysts decreases in the order Al-MCM-41(104) > Al-MCM-41(55) > Al,Zn-MCM-41(52). Similarly pore volume decreases in the same order due to the presence of textural mesoporosity [22].

FT-IR spectra of the as-synthesized and calcined Al-MCM-41 ($\mathrm{Si/Al} = 55$ and 104) and Al,Zn-MCM-41 ($\mathrm{Si/(Al + Zn)} = 52$) molecular sieves are presented in Fig. 3. The broad envelope around 3500 cm^{-1} is due to O–H stretching of water, surface hydroxyl groups, and bridged hydroxyl groups. There are less intense peaks in the spectra of the as-synthesized samples just below 3000 cm^{-1} which are assigned to symmetric and asymmetric stretching modes of the $-\mathrm{CH_2}$ group of the locked-in template. Their corresponding bending mode is observed at 1400 cm^{-1}. The peaks between 500 and 1200 cm^{-1} are assigned to framework vibrations. The intense peak at 1123 cm^{-1} is attributed to the asymmetric stretching of T–O–T groups. The symmetric stretching modes of T–O–T groups are observed around 800 cm^{-1}, and the peak at 460 cm^{-1} is due to the bending mode of T–O–T. The peak at 963 cm^{-1} is assigned to the presence of defective Si–OH groups. The symmetric and asymmetric stretching modes of the $-\mathrm{CH_2}$ group of the template are absent in the spectra of calcined samples. These spectral features resemble those reported by previous workers [23,24].

The results of TGA of Al-MCM-41 ($\mathrm{Si/Al} = 55$ and 104) and Al,Zn-MCM-41 ($\mathrm{Si/(Al + Zn)} = 52$) are illustrated in Fig. 4. DTA traces are shown in the same figure. In all three thermograms, there is an initial weight loss of about 5% below 100 °C due to desorption of water. The second weight loss due to decomposition and desorption of template occurs between 180 and 300 °C. The percentage weight loss is found to 29.7, 41.0, and 35.1% for Al-MCM-41(104), Al-MCM-41(55), and Al,Zn-MCM-41(52), respectively. This clearly demonstrates that a larger amount of aluminum is planted on the channel surface in Al-MCM-41(55) than in Al-MCM-41(104). The weight loss for Al,Zn-MCM-41(52) should be high compared with that Al-MCM-41(55), but the value is smaller. Such a smaller value was also observed for Cu-MCM-41 compared with Si-MCM-41 by Wang et al. [25]. If Zn^{2+} ions are entirely buried inside the framework, the weight loss should be nearly equal to Al-MCM-41(104). But the percentage weight loss is high and hence zinc is not entirely buried inside the mesopore walls.

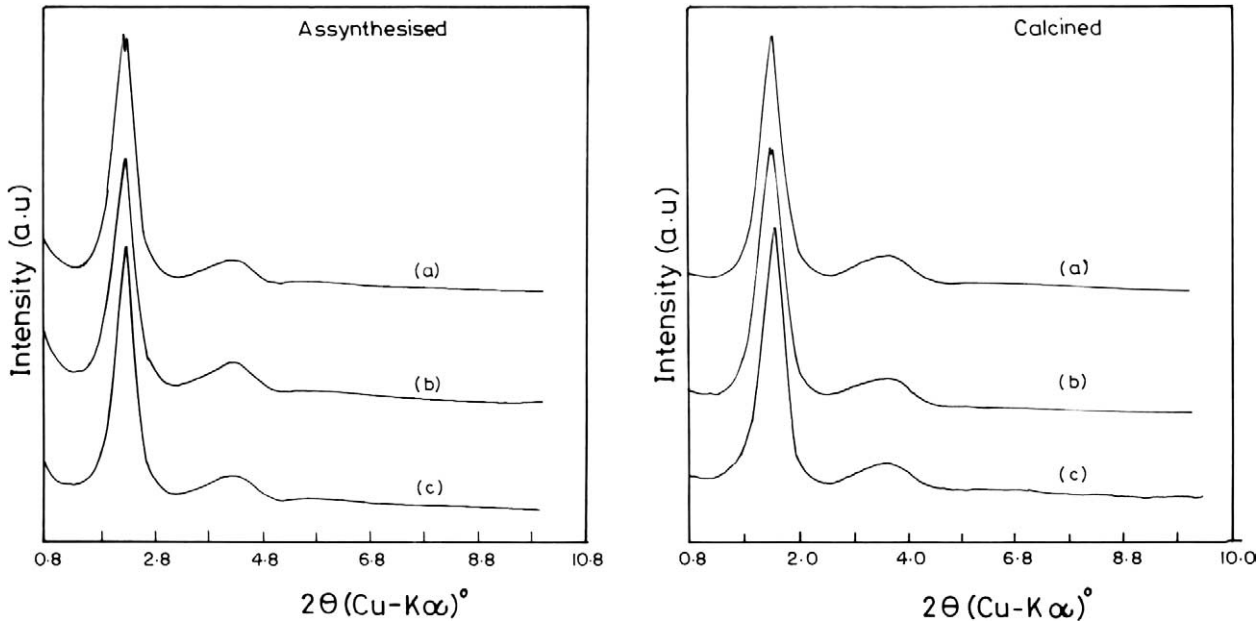

Fig. 1. XRD patterns of as-synthesized and calcined mesoporous Al-MCM-41 molecular sieves: (a) Si/Al = 104, (b) Si/Al = 55, (c) Si/(Al + Zn) = 52.

Table 1
Physical properties of the catalysts

Catalyst[a]	Si/Al		d_{100} (Å)	a_0 (Å)	BET surface area (m^2/g)	Pore volume (cm^3/g)	Pore diameter (nm)	Wall thickness (Å)	^{27}Al MAS-NMR
	Gel ratio	ICP							Al_T/Al_O[b]
1	50	55	41.7	48.2	979	0.68	2.79	20.3	4.1
2	50[c]	52[c]	37.5	43.3	930	0.66	2.57	17.6	7.4
3	100	104	40.6	46.9	1044	0.66	2.83	18.6	∞

[a] (1) Al-MCM-41(55), (2) Al,Zn-MCM-41(52), (3) Al-MCM-41(104).
[b] ^{27}Al MAS-NMR spectra: ratio of the intensities of 4- and 6-coordinated aluminum in the calcined catalysts.
[c] Si/(Al + Zn) ratio.

^{29}Si MAS-NMR spectra of the calcined Al-MCM-41 materials are shown in Fig. 5. The partly resolved signal at −92 ppm is assigned to Q_2 species. This signal is less intense for Al-MCM-41(104) and more intense for Al-MCM-41(55) and Al,Zn-MCM-41(52). The other signals at −101 (Q_3) and −106, −110 (Q_4) appear similar to those reported in the literature [26–28]. ^{27}Al MAS-NMR spectra of the samples are shown in Fig. 6, and the ratio of the intensities of 4- and 6-coordinated aluminum was calculated and is given in Table 1. The peak at 53 ppm in all spectra is assigned to tetrahedrally coordinated framework aluminum, and the peak at 0 ppm is assigned to octahedral nonframework aluminum species [24,25]. Al-MCM-41(104) is devoid of any nonframework Al^{3+} (Al_2O_3) as there is no signal at 0 ppm. But Al-MCM-41(55) and Al,Zn-MCM-41(52) have such species as there is a broad signal at 0 ppm. Generally, materials with high aluminum content are susceptible to framework leaching of aluminum during calcination [28]. In the present study, calcination of the as-synthesized materials was done in air directly without using nitrogen in the beginning. This would also aid framework leaching. Even for those materials of high aluminum content this problem can be avoided by calcining in a nitrogen atmosphere. The absence of octahedral Al^{3+} in Al-MCM-41(104) and the presence of the same in Al-MCM-41(55) are attributed to the high aluminum content of the latter catalyst. But Al,Zn-MCM-41(52) has nearly same Si/Al ratio as Al-MCM-41(104). Hence the peak due to octahedral aluminum in the former cannot be explained on the basis of aluminum content. Reddy et al. [29] have reported preparation of Al-MCM-41 (Si/Al = 104 and 50) materials without any nonframework aluminum using aluminum sulfate as the source. But they reported calcination of the materials in nitrogen prior to air. Hence calcination of the materials exclusively in air and zinc substitution may cause the framework leaching in Al,Zn-MCM-41(52). Chakraborty et al. [30] reported that water-coordinated framework aluminum could also produce the peak at 0 ppm. Van Hooff and coworkers [31] also reported synthesis and characterization of Al-MCM-41, wherein incorporation of an excess of aluminum formed an impure crystal-phase tridimite, and the Lewis acid site prevailed because of the octahedral nonframework aluminum, accompanied by collapse of the structure. As Al-MCM-41(104) contains less aluminum content, the nonframework species is not observed. Al-MCM-41(55) contains more aluminum than Al-MCM-41(104) and Al,Zn-

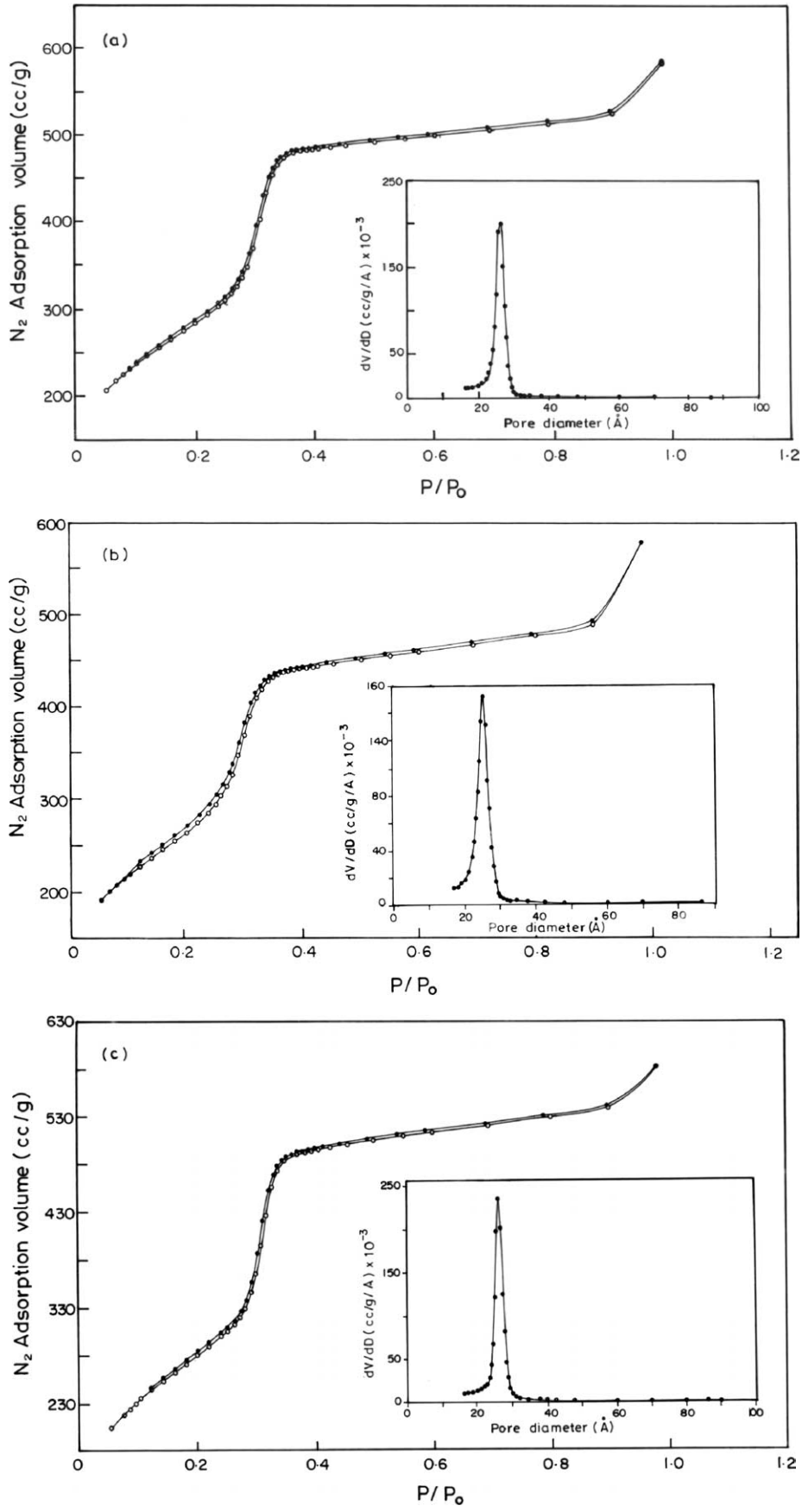

Fig. 2. Adsorption isotherms of Al-MCM-41 molecular sieves: (a) Si/Al = 104, (b) Si/Al = 55, (c) Si/(Al + Zn) = 52.

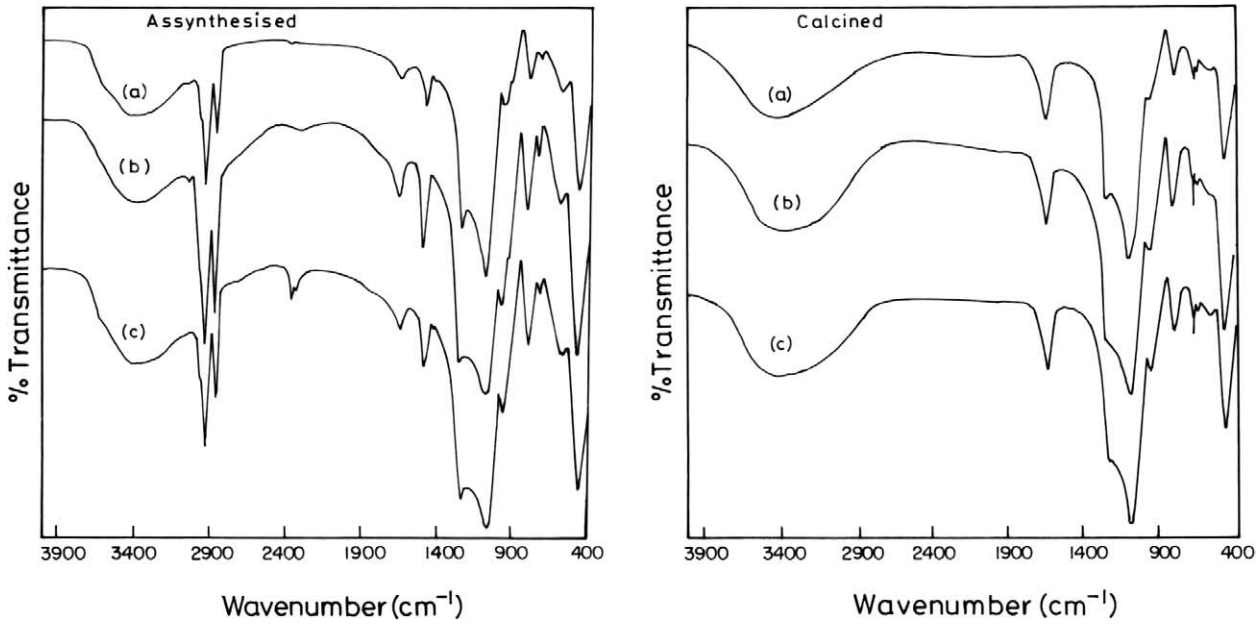

Fig. 3. FTIR spectra of as-synthesized and calcined mesoporous Al-MCM-41 molecular sieves: (a) Si/Al = 104, (b) Si/Al = 55, (c) Si/(Al + Zn) = 52.

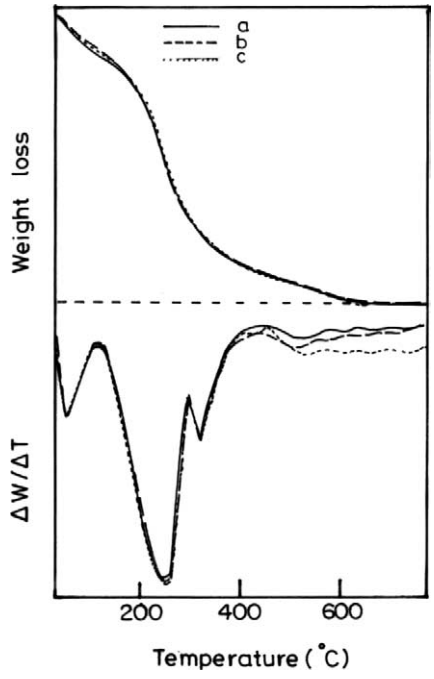

Fig. 4. TGA/DTA analysis of Al-MCM-41 molecular sieves: (a) Si/Al = 104, (b) Si/Al = 55, (c) Si/(Al + Zn) = 52.

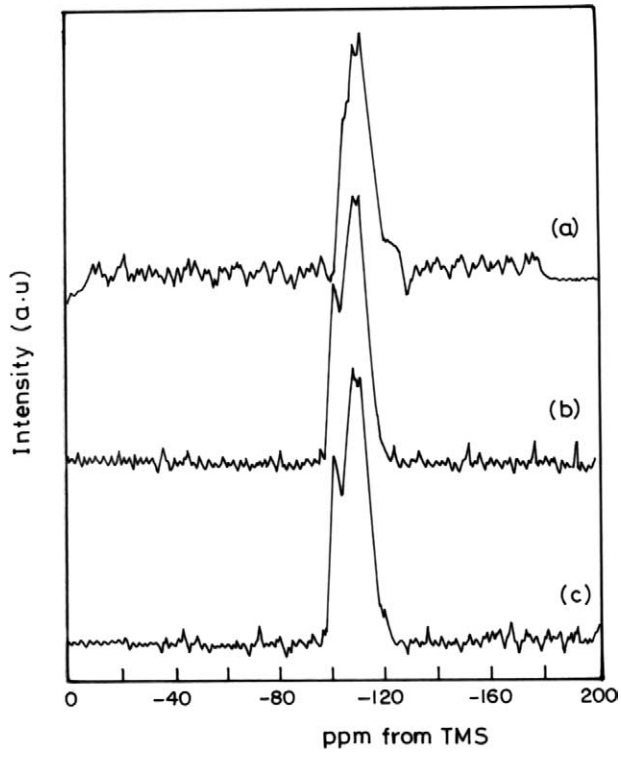

Fig. 5. ^{29}Si MAS-NMR spectra of Al-MCM-41 molecular sieves: (a) Si/Al = 104, (b) Si/Al = 55, (c) Si/(Al + Zn) = 52.

MCM-41(52), and produces a peak due to the octahedral aluminum it contains. The less intense peak at 0 ppm in Al,Zn-MCM-41(52) spectra is due to water-coordinated framework aluminum [30].

The acidity of the calcined materials was measured by FT-IR spectroscopy using pyridine as probe (Fig. 7). The samples give the expected bands due to Lewis acid-bound (1450, 1575, and 1623 cm^{-1}), Brønsted acid-bound (1545 and 1640 cm^{-1}) and both Lewis and Brønsted acid-bound (1490 cm^{-1}) pyridine. These data coincide with those reported by Climent et al. [32]. The acidity of the catalysts was calculated using the extinction coefficients of the bands of Brønsted and Lewis acid site adsorbed pyridine [33] and the results are summarized in Table 2. The data indicate the presence of both Brønsted and Lewis acid sites in Al-MCM-41(55) and Al,Zn-MCM-41(52). These data also coincide

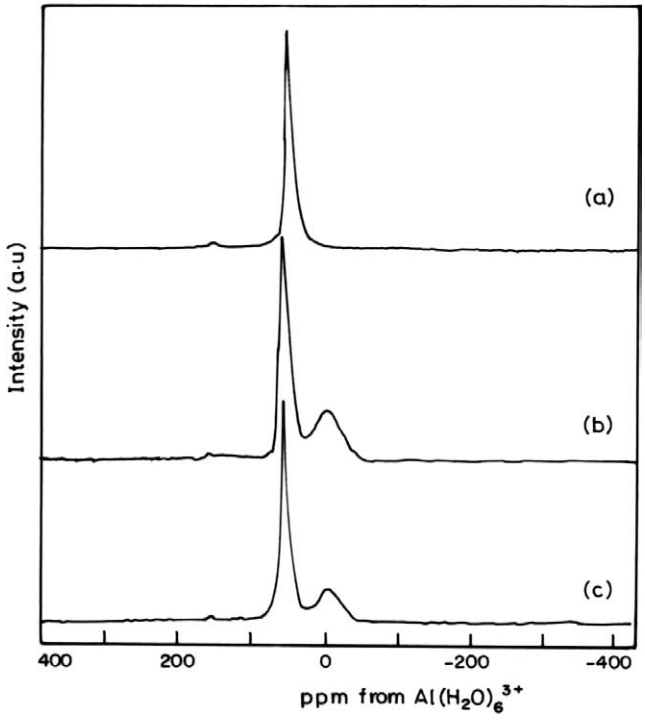

Fig. 6. ^{27}Al MAS-NMR spectra of Al-MCM-41: (a) Si/Al = 104, (b) Si/Al = 55, (c) Si/(Al + Zn) = 52.

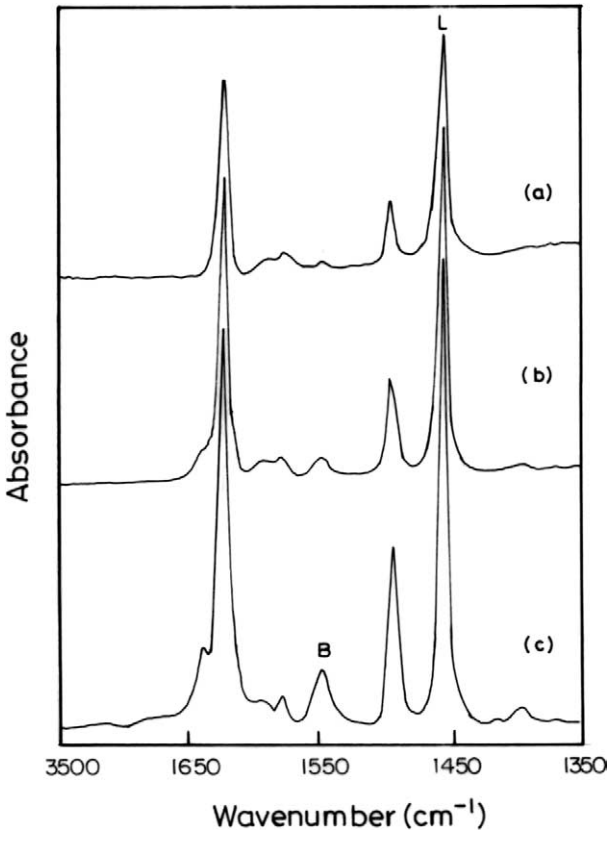

Fig. 7. Brønsted and Lewis acidity of Al-MCM-41: (a) Si/Al = 104, (b) Si/Al = 55, (c) Si/(Al + Zn) = 52.

Table 2
Brønsted and Lewis acidity values for mesoporous molecular sieves

Catalyst	423 K	
	B.A.[a]	L.A.[a]
Al-MCM-41(55)	7.1	9.0
Al,Zn-MCM-41(52)	8.2	9.5
Al-MCM-41(104)	3.7	1.1

[a] Acidity (μmol py/g catalyst).

with the ^{27}Al-MAS-NMR spectra of the catalysts, which indicate the presence of both octahedral and tetrahedral aluminum in Al-MCM-41(55) and Al,Zn-MCM-41(52), but only octahedral aluminum in Al-MCM-41(104). Although the signal due to octahedral aluminum is not observed for Al-MCM-41(104) in ^{27}Al-MAS-NMR (Fig. 6), a slightly smaller amount of Lewis acidity (Table 2) is also observed as reported by Umamaheswari et al. [3].

3.2. Isopropylation of *m*-cresol

Isopropylation of *m*-cresol with isopropyl acetate was investigated over Al-MCM-41(55), Al-MCM-41(104), and Al,Zn-MCM-41(52) in the vapor phase. The effects of reaction temperature, feed ratio, WHSV, and time-on-stream were studied to optimize the parameters for better conversion and selectivity of products.

3.3. Effect of temperature

The influence of reaction temperature on conversion and selectivity was studied at 200, 250, 300, 350, and 400 °C. The reactant feed ratio (*m*-cresol:isopropyl acetate) was maintained at 1:3 and WHSV 1.52 h^{-1}. The products are thymol, isothymol, 2-I-5-MPA, and I-3-MPE (Scheme 1). *m*-Cresol conversion and selectivity of the products at various temperatures are summarized in Table 3. An increase in conversion is observed between 200 and 300 °C. The percentage conversion decreases significantly above 300 °C for all catalysts.

Thymol is formed more selectively than other products at all temperatures studied. The high selectivity of thymol is due to chemisorption of *m*-cresol on the Brønsted acid sites through its –OH group, favoring only *ortho* carbons for reaction with isopropyl cation. As the second and fourth carbons have steric hindrance due to a methyl group, isopropyl cation selectively attacks the sixth carbon to yield thymol. Formation of thymol requires chemisorption of *m*-cresol, but for higher *m*-cresol conversion greater chemisorption of isopropyl acetate is required. The greater than 50% *m*-cresol conversion at all temperatures studied reveals the greater adsorption of isopropyl acetate. Selectivity to isothymol is higher at lower temperatures than at higher temperatures. The formation of isothymol is due to the different configuration of the aromatic ring on the catalyst surface as proposed by Taylor and Ludlum [34]. Isothymol could also be formed via isomerization of thymol over strong acid sites. Thus,

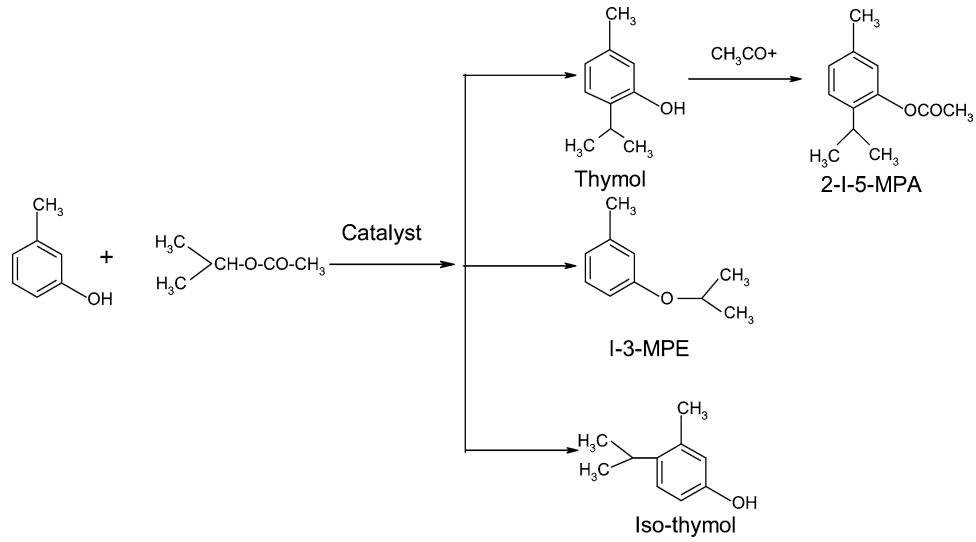

Scheme 1. Reaction of *m*-cresol with isopropyl acetate.

Table 3
Effect of temperature on *m*-cresol conversion and product selectivity[a]

Catalyst	Temperature (°C)	*m*-Cresol conversion (%)	Selectivity of product (%)			
			Thymol	Isothymol	2-I-5-MPA	I-3-MPE
Al-MCM-41(55)	200	68.6	71.7	9.5	3.6	15.2
	250	75.1	76.1	8.5	4.2	11.2
	300	80.9	83.7	4.5	7.9	3.9
	350	70.3	87.9	3.2	5.4	3.5
	400	60.2	91.6	2.0	3.4	3.0
Al,Zn-MCM-41(52)	200	60.1	63.9	9.8	10.7	15.6
	250	65.9	67.6	7.6	11.9	12.9
	300	70.1	70.2	6.6	14.3	8.9
	350	58.6	76.9	5.7	9.2	8.2
	400	50.0	82.4	4.8	5.9	6.9
Al-MCM-41(104)	200	53.7	57.6	13.3	12.7	16.4
	250	56.7	61.2	9.7	14.2	14.9
	300	62.9	63.2	9.0	16.9	10.9
	350	57.9	67.9	8.3	13.2	10.6
	400	49.3	71.9	7.8	11.9	8.4

[a] *m*-Cresol:isopropyl acetate (feed ratio) = 1:3. WHSV = 1.52 h^{-1}.

there are two routes by which isothymol could be formed in this reaction. Isomerization of thymol to isothymol is greater at low temperature (≈200 °C) than at 400 °C as reported by earlier workers [10]. Although isomerization of thymol can occur on the same acid sites that catalyze the formation of thymol, the selectivity to isothymol is low. This suggests that the sites are not acidic enough for isomerization.

Selectivity to 2-I-5-MPA increases up to 300 °C and then decreases. Sakthivel et al. [35] reported the distribution of weak, moderate, and strong acid sites for Al-MCM-41. The weak acid sites were assigned to surface hydroxyls, and the moderate and strong acid sites, to briged hydroxyls. O-Acylation was observed in this study, not C-acylation. O-Acylation is generally considered to occur on defective sites which are less effective for adsorption of *m*-cresol compared with bridged hydroxyl groups. These defective hydroxyl groups can adsorb ester by increasing the polarization of the carbonyl group by weak protonation. The polarization of ester is not sufficient to yield isopropyl cation, but sufficient enough for nucleophilic attack by *m*-cresol diffusing close to it. To verify that O-acylation of *m*-cresol occurs mostly on defective sites of the catalysts, the reaction was studied with Si-MCM-41, which has only defective acid sites. At 300 °C with a feed ratio of 1:3 and a flow rate of 1.5 ml/h, the conversion of *m*-cresol is 47.9%, with the formation of only 2-I-5-MPA thus supporting our view.

To establish that O-acylation is due to partly protonated ester and not acetic acid, which is a by-product formed during the reaction, the study was repeated with acetic acid as one of the reactants with the feed ratio 1:3:1 (*m*-cresol:isopropyl acetate:acetic acid) under similar conditions. The selectivity to 2-I-5-MPA did not vary significantly, thus confirming that it is only the ester that gives O-acylation. The reaction was also studied with acetic acid alone as acylating agent with the feed ratio 1:1 (*m*-cresol:acetic acid) under the same experimental conditions. Selectivity to O-acylation was only 15.8%, suggesting

that acetic acid is a weak acylating agent as reported in the literature [36].

Selectivity to I-3-MPE increases at lower temperatures and gradually decreases with increase in temperature. At 200 °C, the maximum selectivity was found to be only 15%. This again confirms the chemisorbed state of *m*-cresol on the catalyst surface at the 1:3 feed ratio. The more appropriate route for the formation of I-3-MPE is the reaction between *m*-cresol in the vapor phase and isopropyl cation on the catalyst surface. The possibility of conversion of I-3-MPE to thymol is also ruled out as its selectivity is less, even at 200 °C.

The activity of the catalysts follows the order Al-MCM-41(55) > Al,Zn-MCM-41(52) > Al-MCM-41(104). But their acidity follows the order Al,Zn-MCM-41(52) > Al-MCM-41(55) > Al-MCM-41(104) as each zinc site plants two protons on the catalyst surface, in comparison to only one proton for each aluminum site. The collapse of this acidity order toward activity indirectly discloses the fact that acidity is not the only factor controlling the activity of the catalysts. In the previous report on alkylation of *m*-cresol with isopropyl alcohol, Umamaheswari et al. [3] considered the hydrophilic and hydrophobic properties of the channel surface of Al-MCM-41 molecular sieves to account for the nearly similar conversions of *m*-cresol over Al-MCM-41(55) and Al-MCM-41(104) catalysts. Similarly, Climent et al. [32] also considered these properties to account for the activity of the catalysts in the acetalization reaction. Based on these reports it is suggested that Al,Zn-MCM-41(52) is more hydrophilic than Al-MCM-41(55) due to close positioning of Brønsted acid sites. Hence, isopropyl acetate with its hydrophobic properties can diffuse through the pores of Al,Zn-MCM-41(52) away from the inner surface in the absence of any external force. This accounts for the low conversion over Al,Zn-MCM-41(52) compared with Al-MCM-41(55). In a similar way, one can expect higher conversion over Al-MCM-41(104) as it is more hydrophobic than the others. But the conversion is less, which is attributed to the lower density of the acid sites in the catalyst. Even if isopropyl acetate can diffuse through the pores close to the inner surface, *m*-cresol can also compete significantly for chemisorption on the Brønsted acid sites of the catalyst.

As *m*-cresol conversion increases from 200 to 300 °C, there might be an increase in the chemisorption of isopropyl acetate on the Brønsted acid sites with increase in temperature. The low *m*-cresol conversion at 200 °C indicates less adsorption of isopropyl acetate than *m*-cresol. The slow decrease in conversion with increase in temperature could be attributed to the scattered distribution of acid sites of the catalyst that avoids multialkylation leading to coke formation. However, the decrease in conversion above 300 °C is due to blocking of active sites by coke. The catalyst becomes black above 300 °C. But compared with zeolites, the large pore diameter of the catalyst under investigation facilitates rapid diffusion of the reactants and products and thereby maintains higher conversion. From Table 3 it can be inferred that selectivity to thymol is higher with all the catalysts, but the selectivity to other products is low with Al-MCM-41(55) compared with the other two catalysts. Based on these observations Al-MCM-41(55) is selected as a suitable catalyst for the reaction of *m*-cresol with isopropyl acetate in the vapor phase.

3.4. Effect of feed ratio

The effect of feed ratio (*m*-cresol:isopropyl acetate) on *m*-cresol conversion and product selectivity was investigated over Al-MCM-41(55) with the feed ratios 1:1, 1:2, 1:3, and 1:4 at 300 °C and the results are presented in Table 4. *m*-Cresol conversion is found to be less than 30% at a 1:1 feed ratio. This reveals that at low feed ratio only *m*-cresol is more highly adsorbed on the acid sites of the catalyst than isopropyl acetate. The conversion increases with an increase in isopropyl acetate content in the feed and reaches a maximum at a 1:3 feed ratio. The smaller selectivity to thymol at the 1:1 feed ratio compared with other feed ratios is due to isomerization of thymol, as more protonic sites are available for chemisorption. Isothymol selectivity gradually decreases with the increase in isopropyl acetate content in the feed.

The effect of feed ratio on conversion and product selectivity over Al-MCM-41(55) was studied by increasing the *m*-cresol content of the feed. The ratio was varied from 2:1 to 4:1 to 6:1 and the temperature was maintained at 300 °C with a feed rate of 1 ml/h (Table 4). Conversion was almost the same for the 1:1 and 2:1 ratios, but decreased for the 4:1 and 6:1 feed ratios. The nearly identical levels of conversion for the 1:1 and 2:1 feed ratios illustrates the availability of an adequate amount of isopropyl cation. Hence at feed ratios 1:1 and 2:1, the adsorption of isopropyl acetate might not be reduced by *m*-cresol as it is more prone to chemisorption on the catalyst surface than *m*-cresol. But at 4:1 and 6:1, the decrease might be due to preferential adsorption of *m*-cresol over ester. The selectivity to thymol decreases, whereas the selectivity to isothymol increases, with an increase in *m*-cresol content in the feed.

For the feed ratios 1:1, 1:2, 1:3, and 1:4, the selectivity to thymol increases but that of isothymol decreases. But for feed ratios 2:1, 4:1, and 6:1 the reverse trend of a decrease in selectivity to thymol and increase in selectivity to isothymol

Table 4
Effect of feed ratio on *m*-cresol conversion and product selectivity[a]

Feed ratio	*m*-Cresol conversion (%)	Selectivity of product (%)			
		Thymol	Isothymol	2-I-5-MPA	I-3-MPE
1:1	28.9	60.2	21.6	18.2	–
1:2	56.8	64.5	18.7	16.0	0.8
1:3	80.9	68.7	14.5	12.9	3.9
1:4	73.2	70.9	9.4	8.7	11.0
2:1	27.4	67.3	16.1	7.1	9.5
4:1	12.9	58.5	28.6	–	12.9
6:1	11.9	45.8	36.2	–	18.0

[a] Al-MCM-41(55). Temperature = 300 °C. Feed ratio = *m*-cresol:isopropyl acetate.

is observed. It is suggested that the formation of isothymol is due to chemisorption of *m*-cresol on the strong acid sites of the catalysts, which leads to ring deactivation, favoring direct *meta* substitution with respect to the –OH group. Such ring deactivation that facilitates *meta*-substitution has been reported previously [37].

The selectivity to 2-I-5-MPA decreases when the feed ratio changes from 1:1 to 2:1 and disappears at feed ratios 4:1 and 6:1, as its formation requires two consecutive processes of alkylation and acylation. The prevention by the high *m*-cresol content in the feed of two successive processes for a single molecule in different regions of acidity is not easily envisaged. The selectivity to I-3-MPE increases with an increase in the isopropyl acetate content of the feed. The same trend is also observed for feed ratios 2:1, 4:1, and 6:1, for which isopropyl acetate content decreases. The formation of ether requires reaction between chemisorbed isopropyl acetate and free *m*-cresol in the vapor phase. When the feed ratio is changed from 1:1 to 1:2, 1:3, and 1:4, there could be preferential adsorption of isopropyl acetate, thus leaving more *m*-cresol in the vapor phase which aids the formation of ether. The increase in ether selectivity with feed ratios 2:1, 4:1, and 6:1 illustrates that even with these feed ratios, the preferential adsorption of isopropyl acetate is not avoided by the high content of *m*-cresol, thus giving more selectivity to ether. Hence this study clearly demonstrates that at the feed ratio of 1:3, isopropyl acetate has a greater tendency to be chemisorbed on the catalyst surface than does *m*-cresol, and therefore it could be better exploited for both alkylation and acylation.

3.5. Effect of WHSV

The effect of WHSV on conversion and product selectivity was studied at 1.01, 1.52, and 2.02 h^{-1} with the feed ratio 1:3 at 300 °C, and the results are summarized in Table 5. The conversion decreases with increase in WHSV. However, the decrease is only about 10% when the WHSV is increased from 1.01 to 1.52 h^{-1}, whereas the decrease is more than 40% at 2.02 h^{-1}. The drastic decrease in conversion at 2.02 h^{-1}, is due to fast diffusion of *m*-cresol, which is largely retained in the vapor phase by isopropyl acetate. The higher selectivity to thymol was attained at WHSV 2.02 h^{-1}. As isothymol is formed by isomerization of thymol, which is a time-dependent process, its selectivity is high at 1.01 h^{-1}, and then decreases gradually with the increase in WHSV. A similar decrease in selectivity with increase in WHSV is also observed for 2-I-5-MPA and I-3-MPE. As *m*-cresol conversion and selectivity to thymol are optimum at 1.52 h^{-1}, the time-on-stream study was carried out at this WHSV.

Table 5
Effect of WHSV on *m*-cresol conversion and product selectivity[a]

WHSV (h^{-1})	*m*-Cresol conversion (%)	Selectivity of product (%)			
		Thymol	Isothymol	2-I-5-MPA	I-3-MPE
1.01	89.7	60.9	18.4	14.4	6.3
1.52	80.9	68.7	14.5	12.9	3.9
2.02	40.2	80.5	7.7	9.3	2.5

[a] Al-MCM-41(55). Temperature = 300 °C.

3.6. Effect of time-on-stream

The effect of time-on-stream was studied for 5 h over Al-MCM-41(55) at 300 °C with a feed ratio of 1:3 and at WHSV 1.52 h^{-1} (Fig. 8a). There is a rapid decrease in conversion in the first 2 h, which is followed by a slow decrease thereafter. In the beginning of the stream all the sites are free, and hence multialkylation of *m*-cresol leading to coke formation is rapid. But after 2 h on stream, a smaller number of sites are available for activity, and further blocking of the active sites is reduced. Hence there is a slow decrease in conversion. The selectivity to thymol increases with increase in the stream, and the reverse trend in the selectivity to isothymol is observed. At the end of the fourth hour of stream, 2-I-5-MPA and I-3-MPE are not observed. The time-on-stream study also illustrates disappearance of acylated products after 3 h. Acetic acid is a by-product in the use of isopropyl acetate as alkylating agent. Because the present

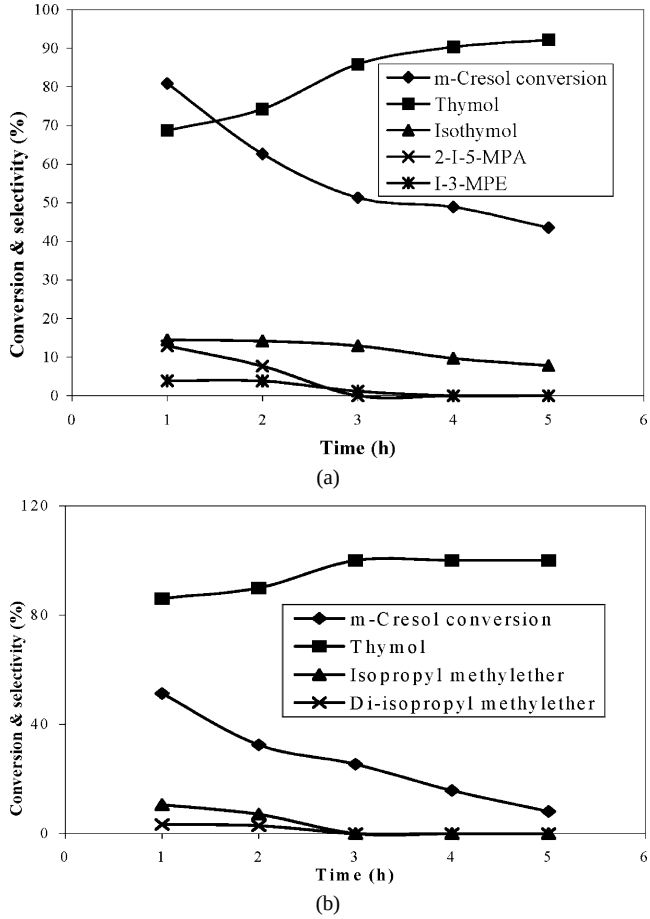

Fig. 8. (a) Study of time-on-stream over Al-MCM-41(55). Feed ratio = 1:3 (*m*-cresol:isopropyl acetate), temperature = 300 °C, and WHSV = 1.52 h^{-1}. (b) Study of time-on-stream over Al-MCM-41(55). Feed ratio = 1:3 (*m*-cresol:isopropyl alcohol), temperature = 300 °C, and WHSV = 1.52 h^{-1}.

investigation involves the use of mesoporous materials, the acetic acid formed in the vapor state easily diffuses out, and hence its tendency to promote coke formation is not as great as that of microporous zeolites.

To compare the activity of isopropyl acetate and isopropyl alcohol in the isopropylation of *m*-cresol, the reaction was also studied with the latter at 300 °C with a feed ratio of 1:3 and a flow rate of 1.5 ml/h. *m*-Cresol conversion is found to be 51% at 1 h, which is about 29% less than that of isopropyl acetate. This observation proves that isopropyl acetate is a better alkylating agent than isopropyl alcohol. As discussed previously the ease of adsorption at the steric free carbonyl group of the ester might be the reason for the enhanced conversion. The effect of time-on-stream with isopropyl alcohol was also studied, and the results are illustrated in Fig. 8b. Conversion decreases with stream in the first 3 h and remains almost constant thereafter, whereas the time-on-stream study with isopropyl acetate indicates a rapid decrease in conversion in the first 3 h on stream, followed by a slow decrease afterward. Although the conversion is better with isopropyl acetate than isopropyl alcohol, the selectivity to thymol is better with isopropyl alcohol than isopropyl acetate. At the end of 3 h on stream, 100% selectivity to thymol is obtained with 25% *m*-cresol conversion with isopropyl alcohol. But isopropyl acetate gives 85.9% selectivity to thymol with 51.3% *m*-cresol conversion. Though there is a marginally higher selectivity to thymol with isopropyl alcohol, the conversion of *m*-cresol is more than doubled with isopropyl acetate. The major component that increases thymol selectivity with isopropyl alcohol is due to the formation of by-product water, which may deactivate the Brønsted acid sites of the catalysts, thus preventing isomerization of thymol to isothymol.

4. Conclusion

The reaction results allow us to conclude that conversion and selectivity to thymol are greater at higher temperatures. Moderate and strong acid sites promote alkylation, while weak acid sites and silanol defects favor O-acylation. Although acetic acid is one of the by-products, it is not as reactive as ester for acylation. The reaction depends not only on the acid sites of the catalysts; their hydrophilic and hydrophobic properties also play an important role. Al,Zn-MCM-41(52), with a greater density of acid sites than Al-MCM-41(55), is less active due to its more hydrophilic nature. The study reveals that isopropyl acetate can be used as a convenient alkylating agent in the isopropylation of *m*-cresol in the vapor phase over Al-MCM-41 molecular sieves.

Acknowledgment

The authors express their sincere thanks for the generous financial support in the form of a project sponsored by the Department of Science and Technology (DST), Government of India, New Delhi.

References

[1] M. Nitta, Bull. Chem. Soc. Jpn. 47 (1974) 2360.
[2] R. Stroh, R. Seydel, W. Hahn, in: W. Forest (Ed.), Newer Methods of Preparative Organic Chemistry, vol. 2, Academic Press, New York, 1963, p. 337.
[3] V. Umamaheswari, M. Palanichamy, V. Murugesan, J. Catal. 210 (2002) 367.
[4] J.C. Leffingwell, R.E. Shackelford, Cosmet. Perfumery 89 (6) (1974) 69.
[5] R. Hopp, Recent Adv. Tobacco Sci. 19 (1993) 46.
[6] P.L. Teissedre, A.L. Waterhouse, J. Agric. Food Chem. 48 (2000) 3801.
[7] E.L. Krause, W. Ternes, Eur. Food Res. Technol. 209 (1999) 140.
[8] N.V. Yanishlieva, E.M. Marinova, M.H. Gordon, V.G. Raneva, Food Chem. 64 (1999) 59.
[9] M. Milos, J. Mastelic, I. Jerkovic, Food Chem. 71 (2000) 79.
[10] H. Grabowska, J. Wrzyszcz, Res. Chem. Intermed. 27 (2001) 281.
[11] S. Velu, S. Sivasanker, Res. Chem. Intermed. 24 (1998) 657.
[12] T. Yamanaka, Bull. Chem. Soc. Jpn. 49 (1976) 2669.
[13] H.G. Franc, J.W. Stadelhofer, in: Industrial Aromatic Chemistry, Springer-Verlag, Berlin/Heidelberg, 1998, p. 168.
[14] W. Biedarmann, H. Koller, K. Wedemeyer, US patent 4086283 (1978).
[15] P. Wimmer, H.J. Buysch, L. Puppe, US patent 5030770 (1991).
[16] A. Klein, K. Wedemeyer, Bayer DE-OS 2242628 (1972).
[17] V. Umamaheswari, M. Palanichamy, Arabindoo Banumathi, V. Murugesan, Indian J. Chem. A 39 (2000) 1241.
[18] J.S. Beck, J.C. Vartuli, W.J. Roth, M.E. Lernowicz, C.T. Kresge, K.D. Schmitt, C.T.W. Chu, D.H. Olson, E.W. Sheppard, S.B. McCullen, J.B. Higgins, J.C. Schlenker, J. Am. Chem. Soc. 121 (1992) 10834.
[19] J.H. Kin, M. Tanabe, M. Niwa, Micropor. Mater. 10 (1997) 85.
[20] M.L. Ocelli, S. Biz, A. Auroux, G.J. Ray, Micropor. Mesopor. Mater. 26 (1998) 193.
[21] S.J. Greggand, K.S.W. Sing, in: Adsorption, Surface Area and Porosity, 2nd edition, Academic Press, New York, 1982.
[22] T.R. Pauly, Y. Liu, T.J. Pinnavaia, S.J.L. Billinge, T.P. Rieler, J. Am. Chem. Soc. 121 (1992) 8835.
[23] C.Y. Chen, H.X. Li, M.E. Davis, Micropor. Mater. 2 (1993) 17.
[24] S. Biz, M.L. Occelli, Catal. Rev. Sci. Eng. 40 (1998) 329.
[25] L. Wang, S. Velu, S. Tomura, F. Ohashi, K. Suzuki, M. Okazaki, T. Osaki, M. Maeda, J. Mater. Sci. 37 (2002) 801.
[26] A. Corma, Micropor. Mesopor. Mater. 4 (1997) 249.
[27] Y. Sun, Y. Yue, Z. Gao, Appl. Catal. A 161 (1997) 121.
[28] A. Matsumoto, H. Chen, K. Tsutsumi, M. Grun, K. Unger, Micropor. Mesopor. Mater. 32 (1999) 55.
[29] K.M. Reddy, C. Song, Catal. Today 31 (1996) 137.
[30] B. Chakraborty, B. Viswanathan, Catal. Today 49 (1999) 253.
[31] M. Busio, J. Janchen, J.H.C. Van Hooff, Micropor. Mater. 37 (2002) 801.
[32] M.J. Climent, A. Corma, S. Iborra, S. Miquel, J. Primo, F. Rey, J. Catal. 183 (1999) 76.
[33] C.A. Emies, J. Catal. 141 (1993) 347.
[34] D.R. Taylor, K.H. Ludlum, J. Phys. Chem. 76 (1972) 2882.
[35] A. Sakthivel, S.K. Badamali, P. Selvam, Micropor. Mesopor. Mater. 39 (2000) 457.
[36] P. Botella, A. Corma, J.M. Lopez-Nieto, S. Valencia, R. Jacquot, J. Catal. 195 (2000) 79.
[37] B. Rajesh, M. Palanichamy, V. Kazansky, V. Murugesan, J. Mol. Catal. A 187 (2002) 259.